Table S1. Criteria used for filtering GEDI data

Description	**Justification**
Dropped the points with quality_flag = 0	Guarantees good waveform quality
Observations limited to nighttime (solar elevation ≤ 0 degrees)	Mitigates influence of background noise from reflected solar radiation
Dropped the points with degrade_flag = 0	Avoids potential geolocation errors under suboptimal conditions
Dropped the points with footprint slope > 20 degrees	Prevents inaccuracies in vegetation height on steep terrain. Slope is determined by the Shuttle Radar Topography Mission (SRTM) data (see GEE code).
Dropped the points with urban_proportion > 5%	Focuses on non-urbanized forest settings
Dropped the points with landsat_water_persistence = 0	Eliminates areas with consistent water coverage
Dropped the points with landsat_tree_cover < 10%	Confirms significant forest canopy presence
Dropped the points with rh98 > 100 m	Maintains focus on typical forest canopy heights, avoiding outliers
Dropped the points with rh50 ≤ 0 m	Confirms presence of vertical structure in vegetation
Dropped the points with total canopy cover ≤ 0.1	Indicates significant presence of canopy materials
Dropped the points with leaf-off_flag ≠ 0	Ensures data represents vegetation during growing season, avoiding underestimation of structural complexity in deciduous trees
Dropped the points with num_detectedmodes = 0	A signal without modes is indicative of pure noise, lacking information on forest vertical structure
Dropped the points with surface_flag = 0	Ensures presence of ground returns in waveform, essential for accurate vertical structure determination
Dropped the points with sensitivity < 0.95	Provides high confidence in proper representation of forest's vertical structure

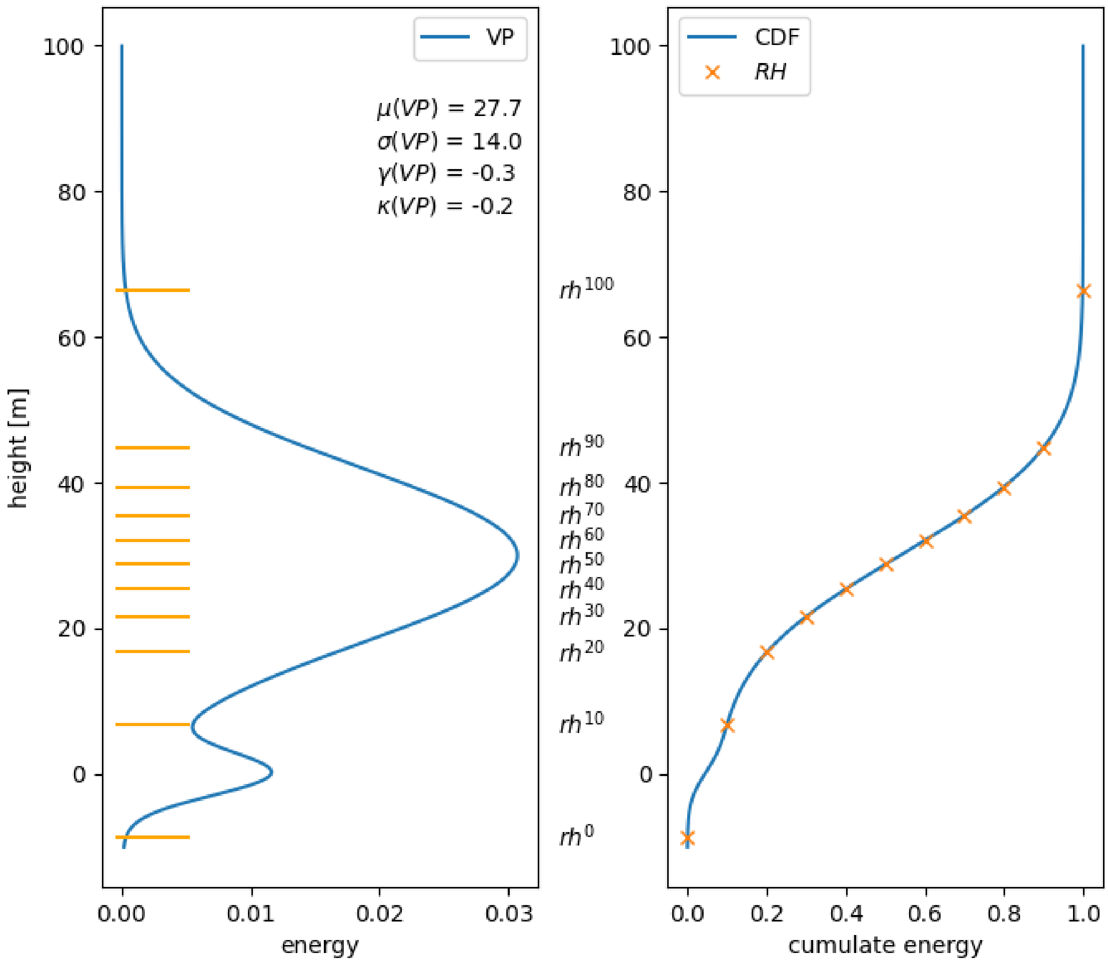

Figure S1. Vegetation vertical profile (denoted as VP) as detected by GEDI waveform (left panel). The numbers within the first panel indicate the four moments (for notation see Appendix A1 main text). The second panel shows the corresponding cumulative distribution function (CDF) of the relative heights (RH) (right panel).

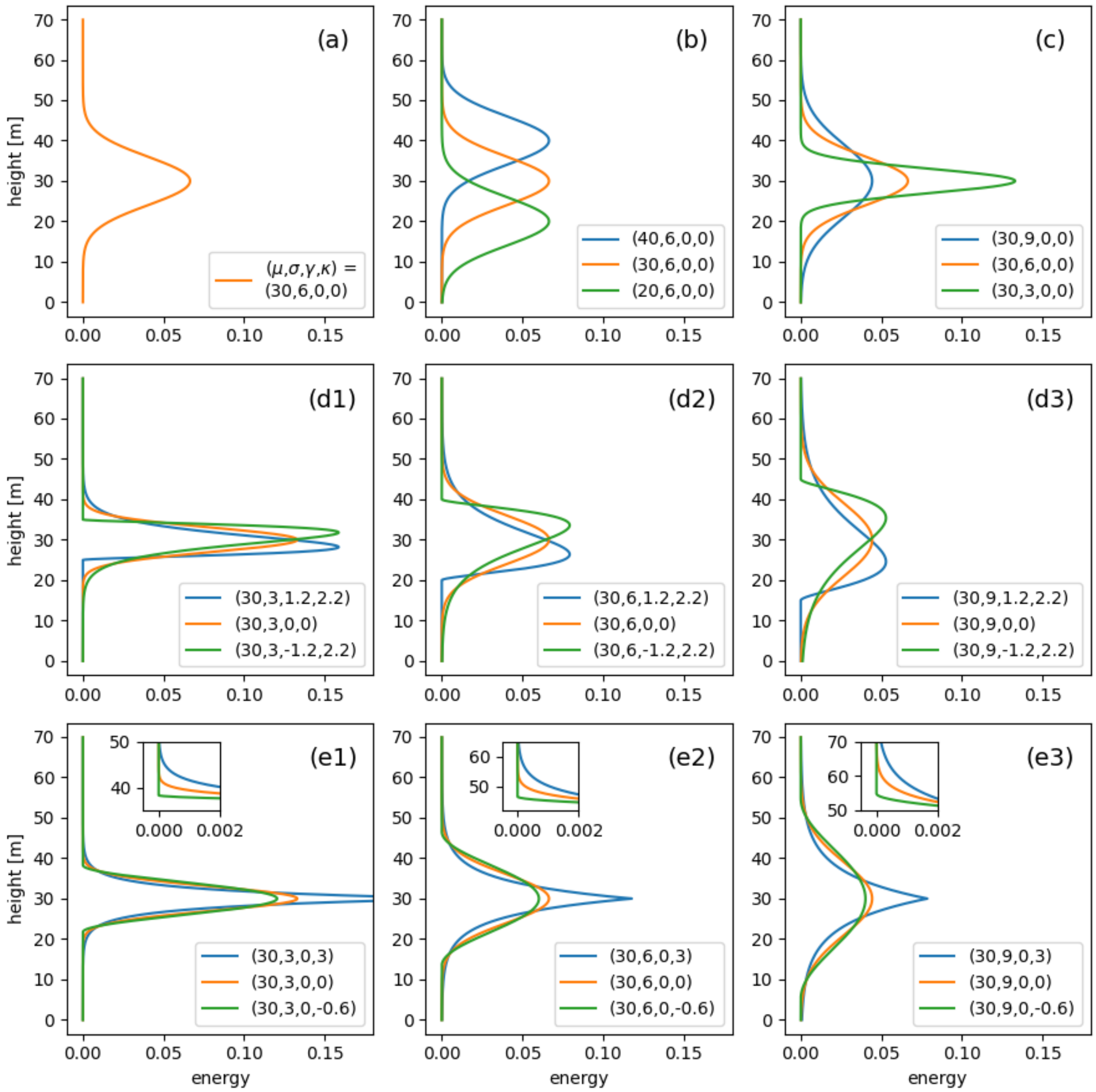

Figure S2. Examples of different unimodal vertical profiles and their relative moments μ, σ, γ, κ. Panel (a): $\mu = 30$, $\sigma = 6$, $\gamma = 0$, and $\kappa = 0$ (i.e. normal distribution). Panel (b): variation of μ (20, 30, 40 m) with fixed σ (6 m), fixed γ (0), and fixed κ (0). Panel (c): variation of σ (3, 6, 9 m) with fixed μ (30), fixed γ (0), and fixed κ (0). Panels d: variation of γ (-1.2, 0, 1.2) with fixed μ (30 m), fixed κ (2.2), and σ equal 3 m (panel d1), 6 m (panel d2), and 9 m (panel d3). Panels e: variation of κ (-0.6, 0, 3) with fixed μ (30 m), fixed γ (0), and σ equal 3 m (panel e1), 6 m (panel e2), and 9 m (panel e3).

Table S2. List of the remote sensing predictors used for Random Forest Modelling. $\beta =$ SM stands for spatial mean. $\beta =$ ASM, ENT, DISS stands for the texture metrics Angular Second Moment (ASM), entropy (ENT), and dissimilarity (DISS) index, respectively, see Section 1 in the main text for more details. S1, S2, and AP2 stands for Sentinel-1, Sentinel-2 and AlOS-PULSAR-2, respectively.

Predictor	**Description**	β	**Composite**	**SRS**
$\phi_{S1VVgs\mu}^{\beta}, \phi_{S1VHgs\mu}^{\beta}$	Growing season VV and VH mean	SM, ASM, ENT, DISS	Six-month	
$\phi_{S1VVgs\sigma}^{\beta}, \phi_{S1VHgs\sigma}^{\beta}$	Growing season VV and VH standard deviation	SM	Two-month	
$\phi_{S1VVpre\mu}^{\beta}, \phi_{S1VHpre\mu}^{\beta}$	Pre-peak growing season mean	SM	Two-month	S1
$\phi_{S1VVact\mu}^{\beta}, \phi_{S1VHact\mu}^{\beta}$	Peak growing season mean	SM	Two-month	
$\phi_{S1VVpost\mu}^{\beta}, \phi_{S1VHpost\mu}^{\beta}$	Post-peak growing season mean	SM	Two-month	
ϕ_{CO}^{β}	Coherence 12 days summer	SM	Summer	
$\phi_{AP2HH}^{\beta}, \phi_{AP2HV}^{\beta}$	Annual HH and HV	SM, ASM, ENT, DISS	Annual	AP2
ϕ_{NDVI}^{β}	Normalized difference vegetation index	SM, ASM, ENT, DISS	Six-month	
$\phi_{NDVI\sigma}^{\beta}$	Normalized difference vegetation index standard deviation	SM	Six-month	
ϕ_{NDWI}^{β}	Normalized difference water index	SM, ASM, ENT, DISS	Six-month	S2
ϕ_{NDRE}^{β}	Normalized difference red edge index	SM, ASM, ENT, DISS	Six-month	
ϕ_{MSAVI}^{β}	Modified soil adjusted vegetation index	SM, ASM, ENT, DISS	Six-month	
ϕ_{GNDVI}^{β}	Green normalized vegetation index	SM, ASM, ENT, DISS	Six-month	

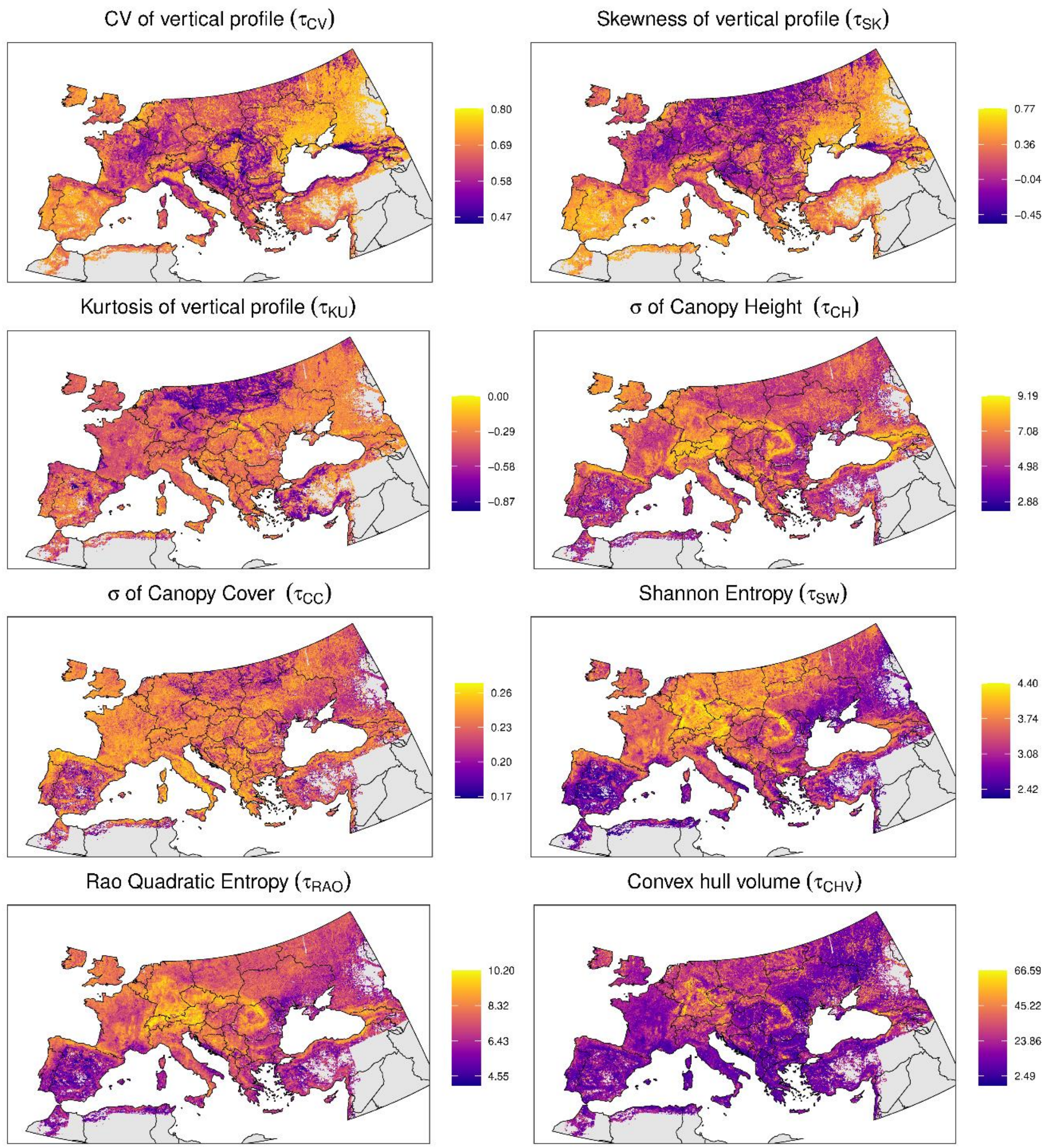

Figure S3 Predicted structural diversity at a 5 km resolution, derived from the Random Forest modelling. Each panel illustrates the geographic distribution of a specific metric (see methods for metric details). The colour palette transitions from purple to yellow, denote an increasing gradient of structural diversity, with warmer colours signifying higher values.

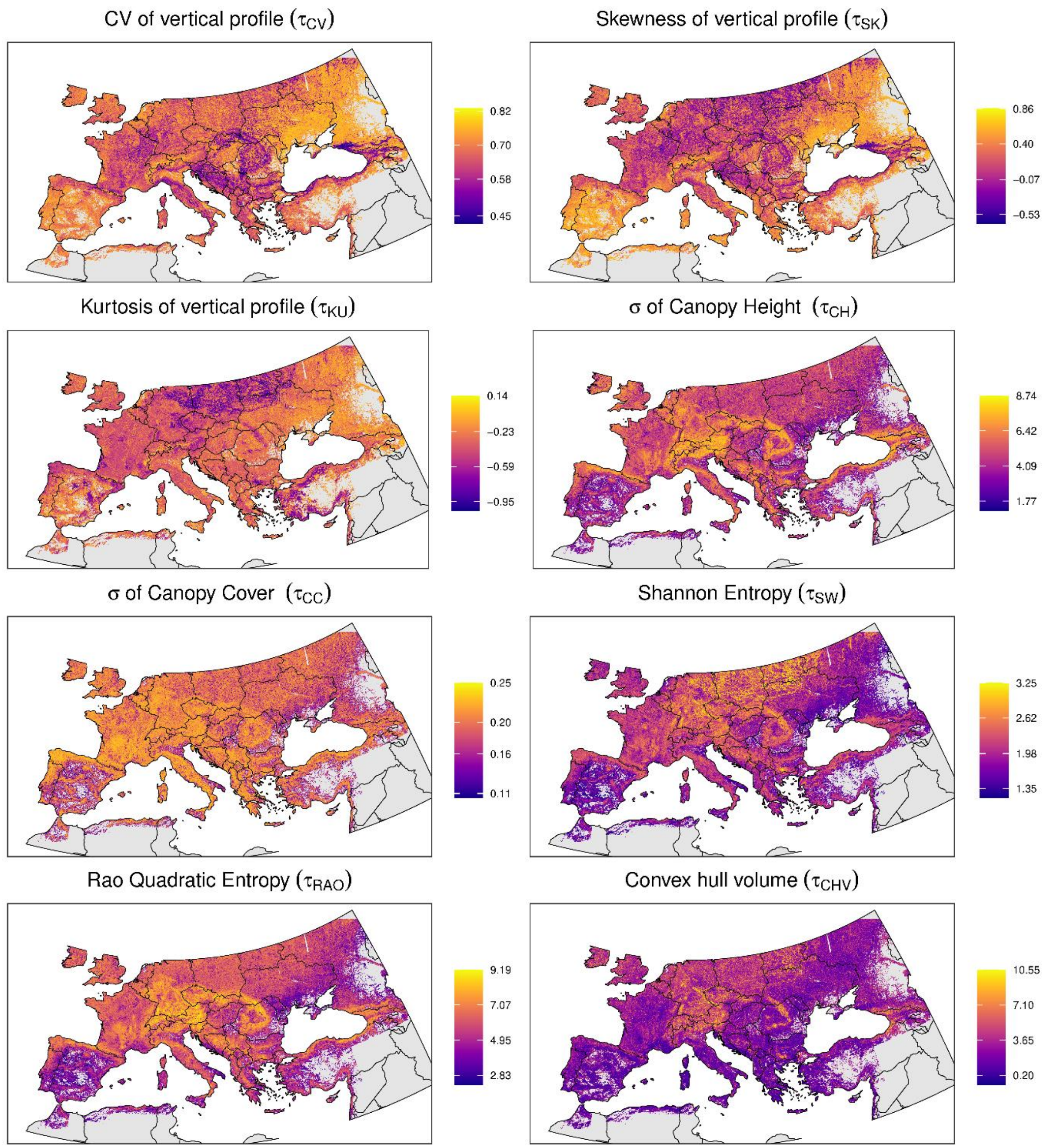

Figure S4 Predicted structural diversity at a 1 km resolution, derived from the Random Forest modelling. Each panel illustrates the geographic distribution of a specific metric (see methods for metric details). The colour palette transitions from purple to yellow, denote an increasing gradient of structural diversity, with warmer colours signifying higher values.

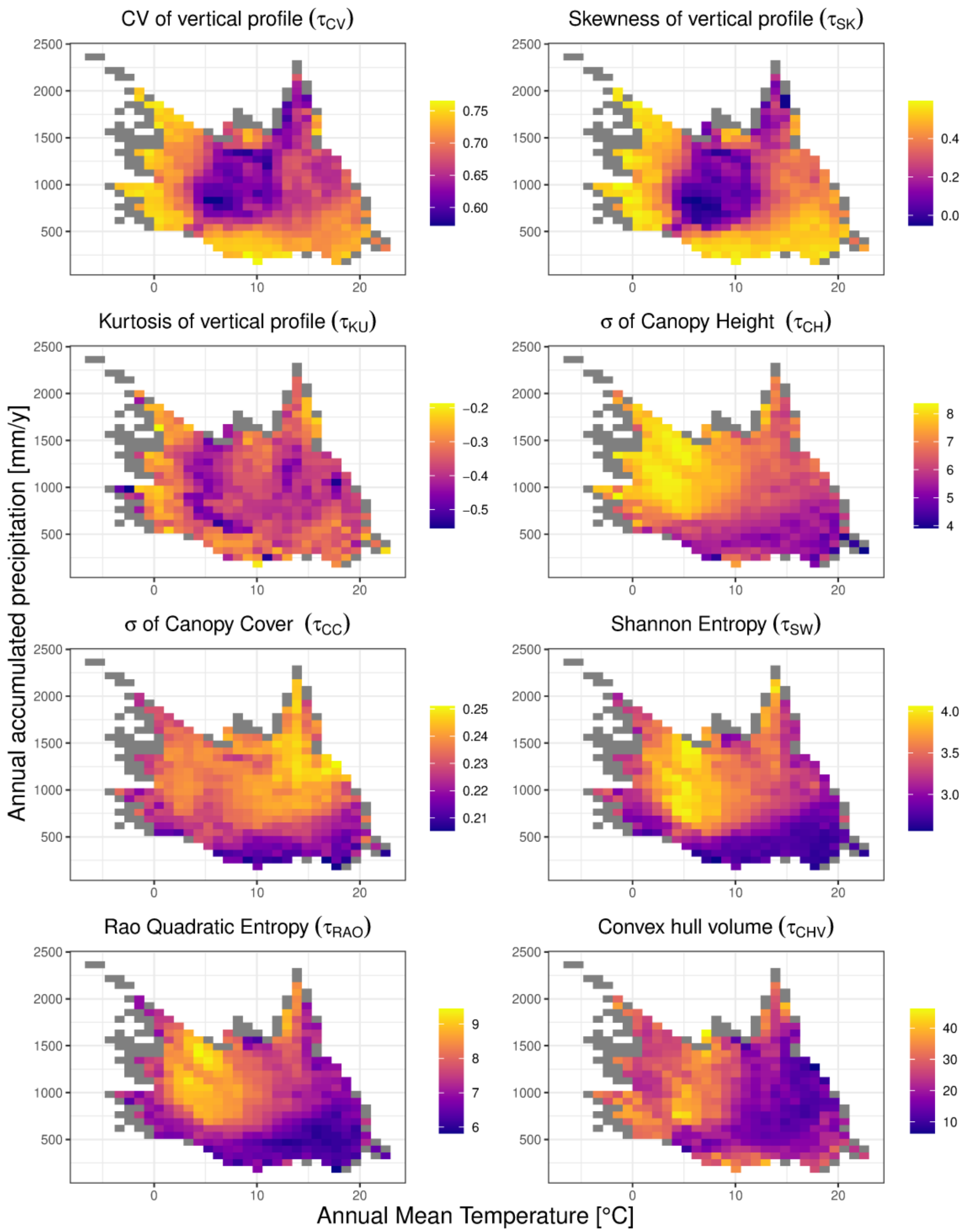

Fig. S5 Predicted structural diversity variables in climate coordinates. The results refer to the dataset at 5 km resolution.

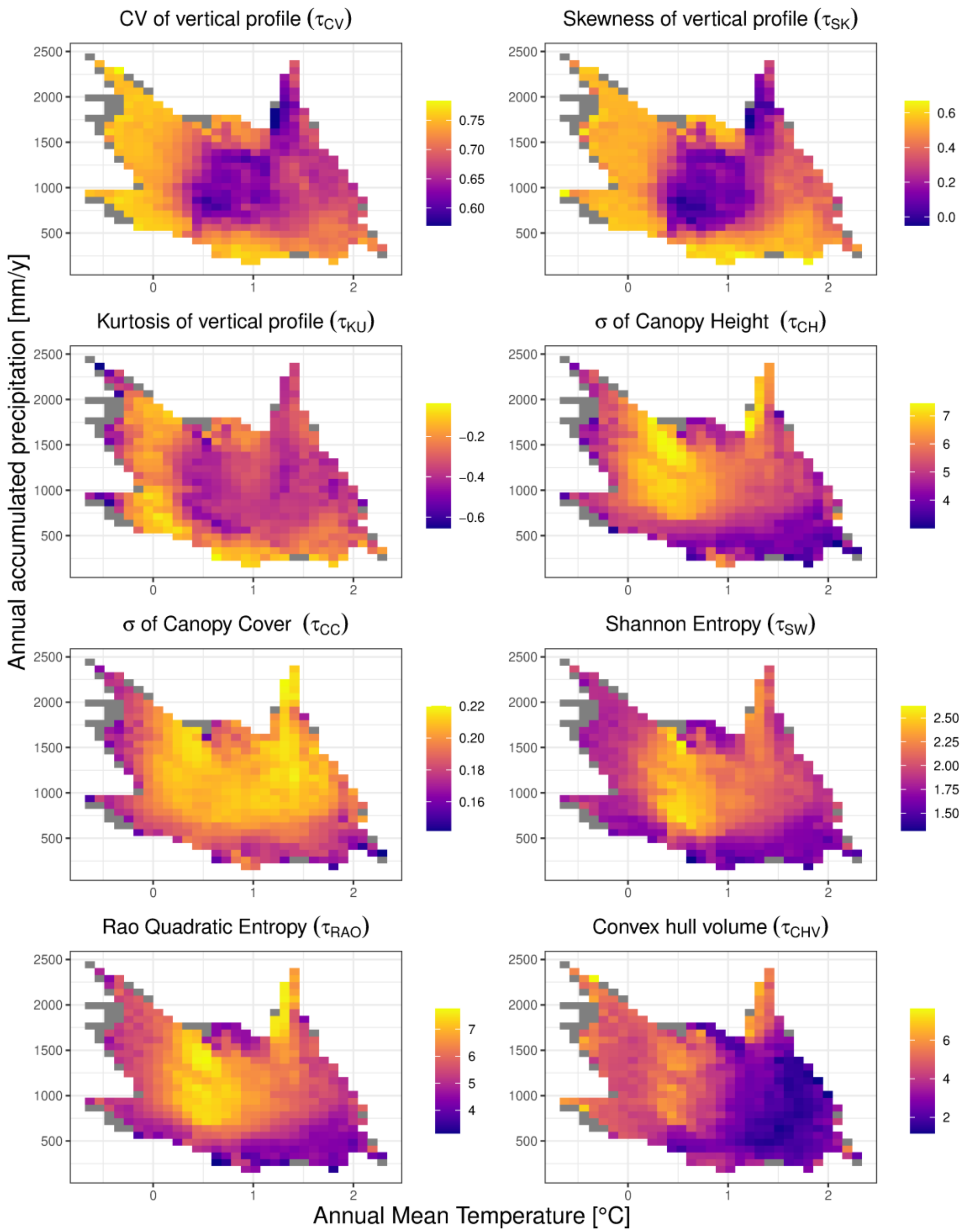

Fig. S6 Predicted structural diversity variables in climate coordinates. The results refer to the dataset at 1 km resolution.

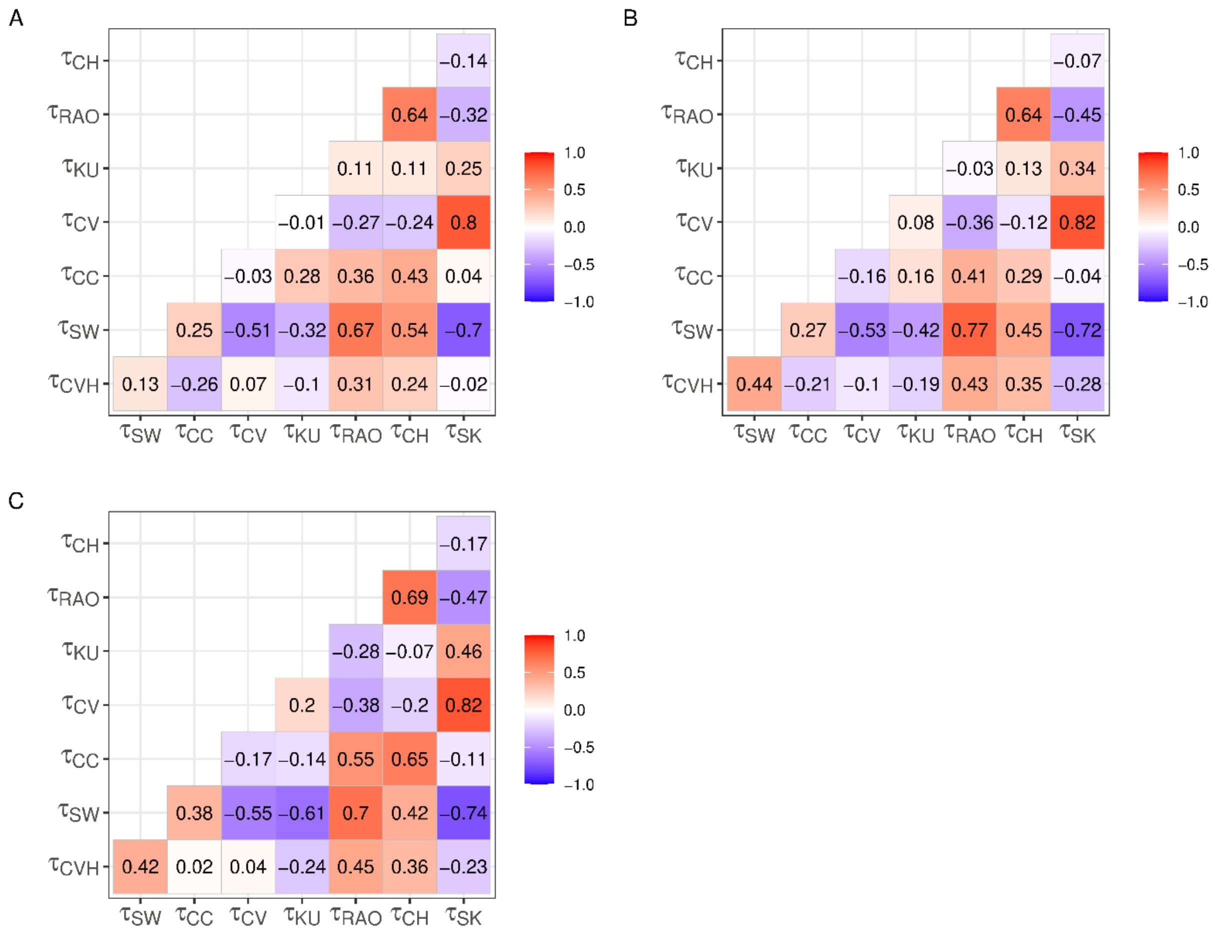

Figure. S7 Pairwise correlations for predicted structural diversity indices. Panel A shows the correlations among indices predicted at a 10 km x 10km resolution, Panel B at a 5km x 5km resolution, and Panel C a 1km x 1km. Each heatmap visualises the interrelationships of structural diversity indices derived from the Random Forest model, highlighting variations across resolutions.

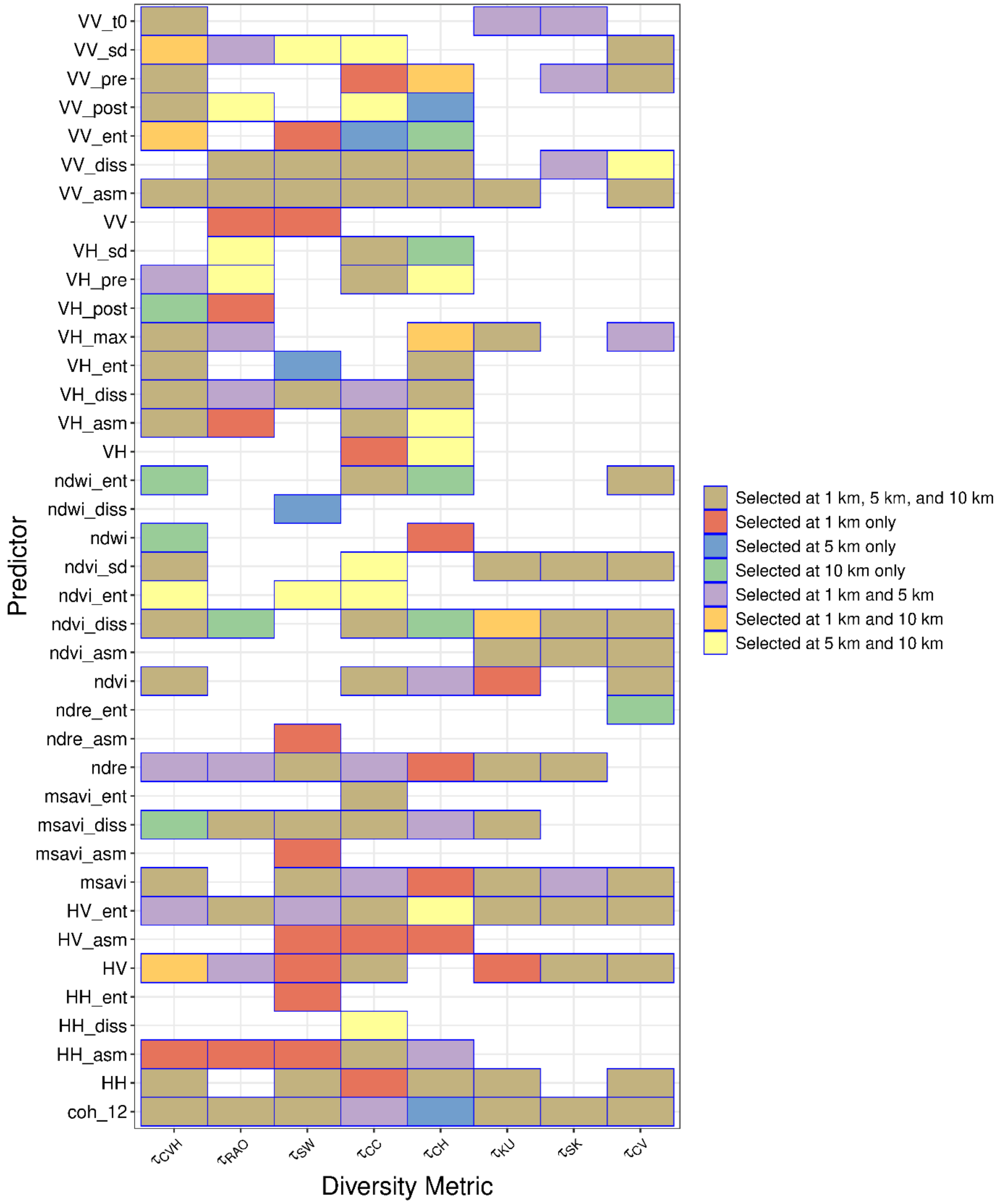

Figure S8 Summary of model selection results using 47 predictors as input variables for models fitted to 8 diversity metrics at different resolutions (1 km, 5 km, 10 km). The y-axis shows the predictors, and the x-axis shows the diversity metrics. Colours indicate whether a specific predictor was selected at one or more resolutions.

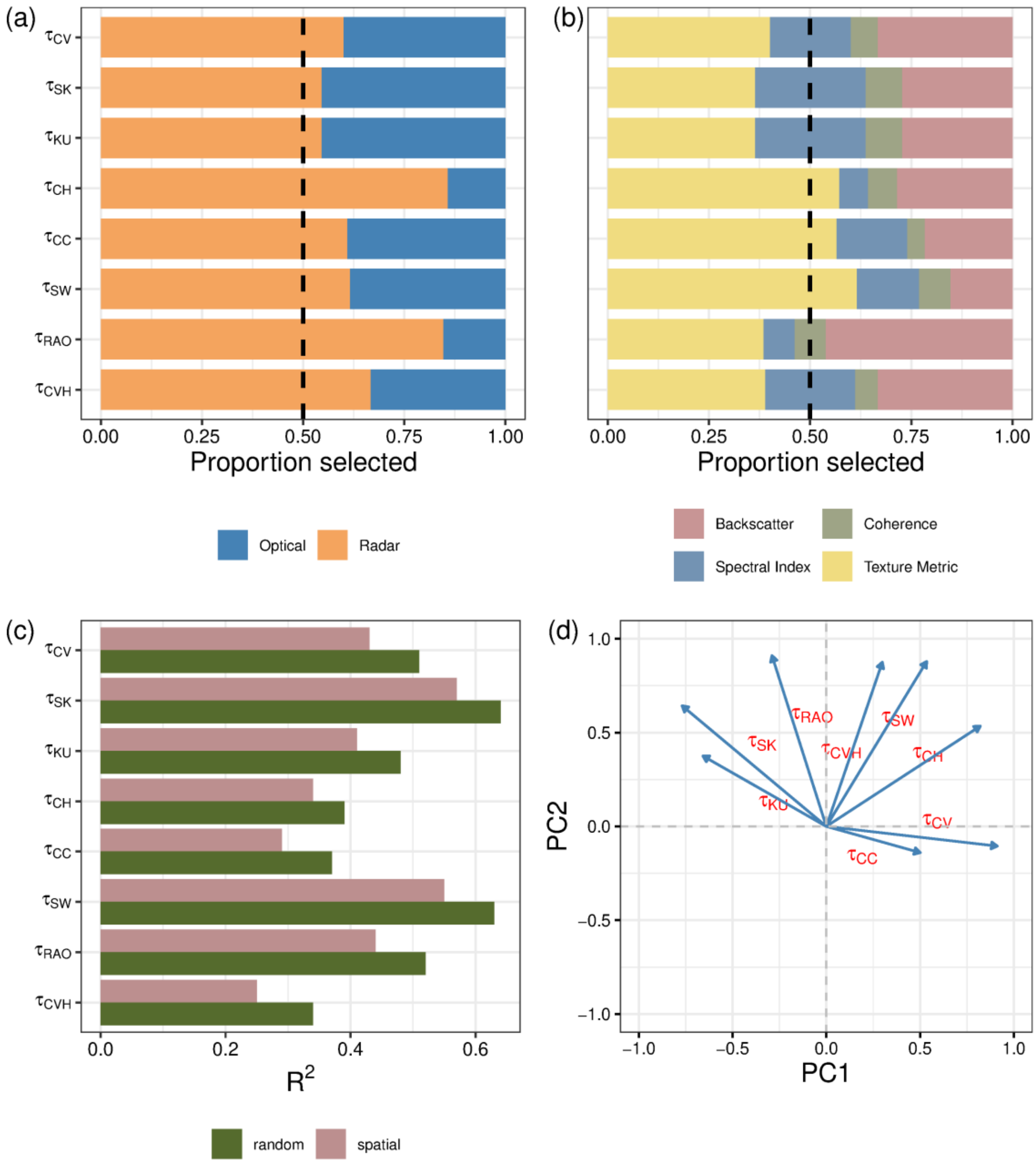

Figure S9. Results from the random forest modelling exercise at 5 km resolution. Panels display the variable selection frequencies (A and B) and model performance, as indicated by the R^2 values derived from two types of validation methods (C). Panel D shows the results of the Principal Component Analysis (PCA) conducted on the predicted metrics at this resolution.

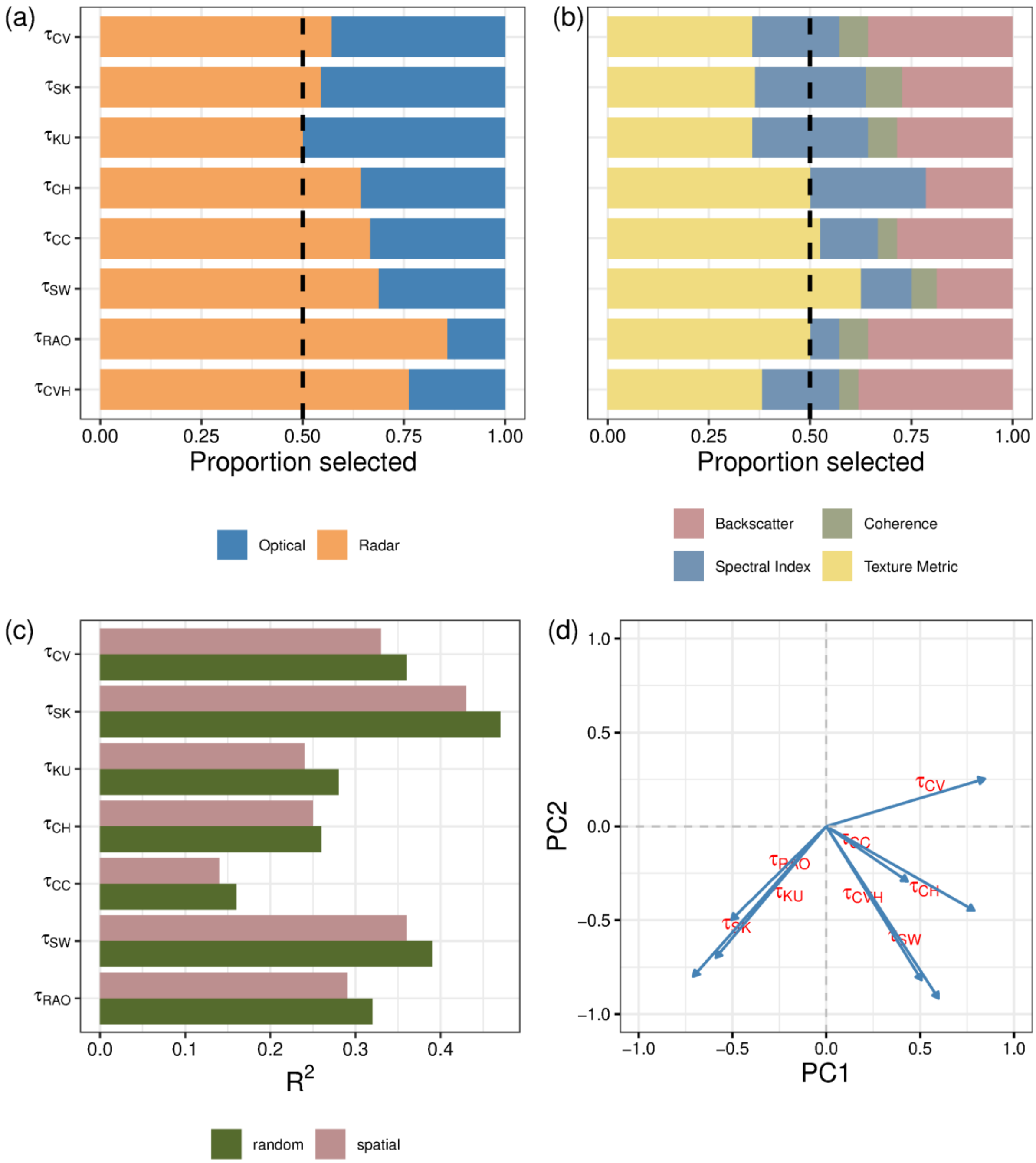

Figure S10 Results from the random forest modelling exercise at 1 km resolution. Panels display the variable selection frequencies (A and B) and model performance, as indicated by the R^2 values derived from two types of validation methods (C). Panel D shows the results of the Principal Component Analysis (PCA) conducted on the predicted metrics at this resolution.

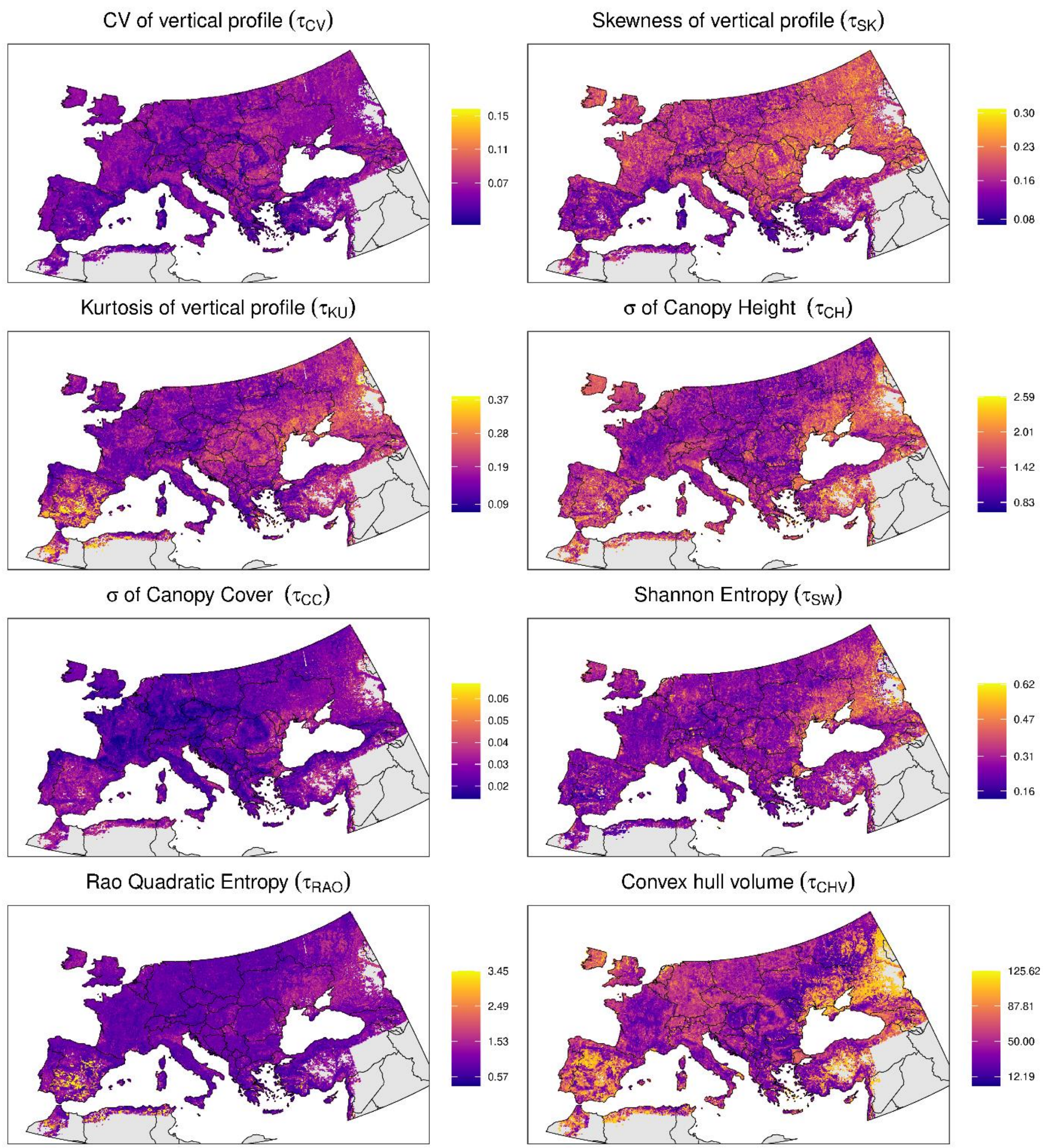

Figure S11. Standard errors of predictions for models trained at 10 km resolution using Random Forest modelling. These errors were calculated using the infinitesimal jackknife method (see Methods for details). The colour palette transitions from purple to yellow, denoting increasing standard error, with warmer colours signifying higher values.

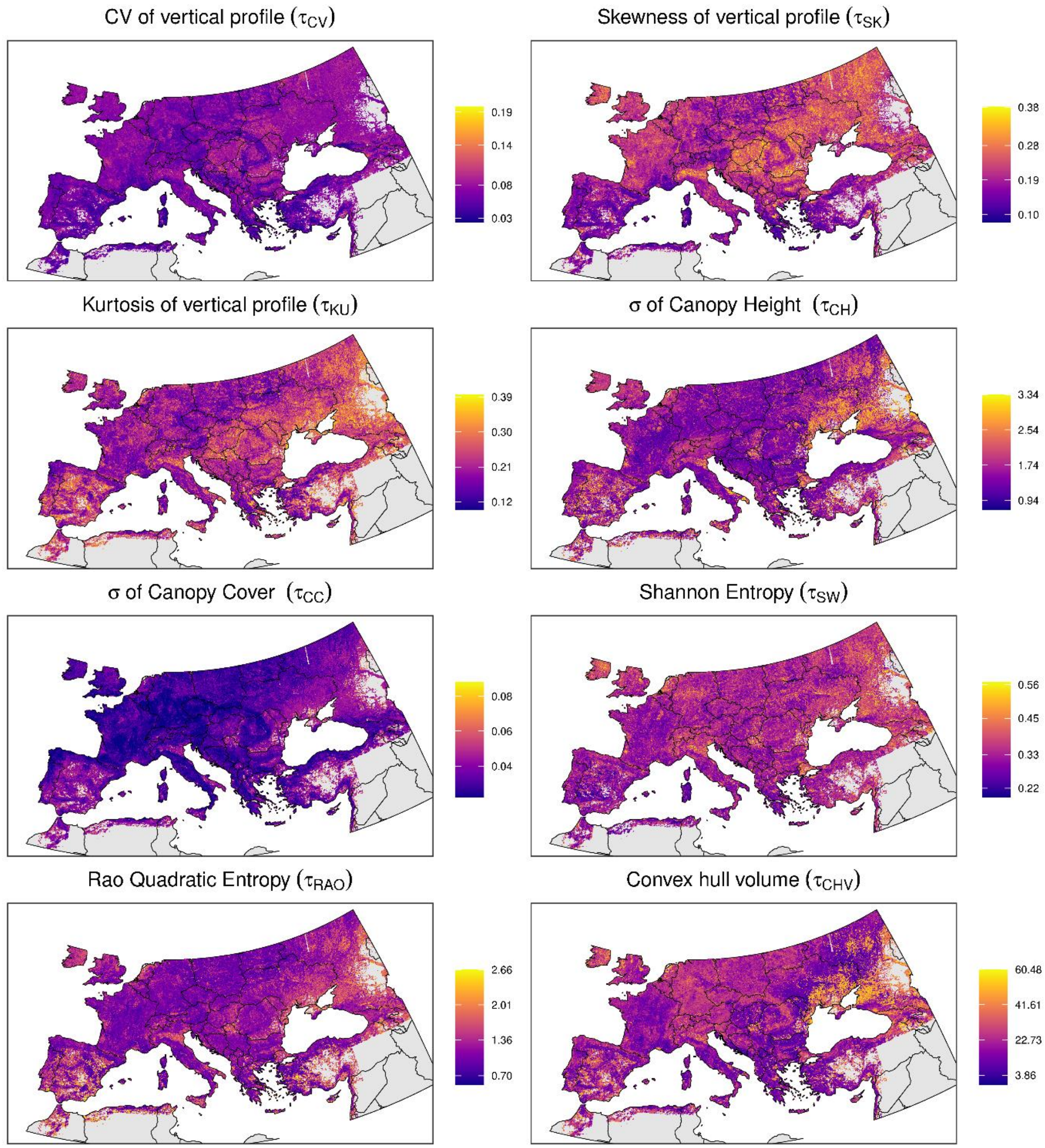

Figure S12 Standard errors of predictions for models trained at 5 km resolution using Random Forest modelling. These errors were calculated using the infinitesimal jackknife method (see Methods for details). The colour palette transitions from purple to yellow, denoting increasing standard error, with warmer colours signifying higher values.

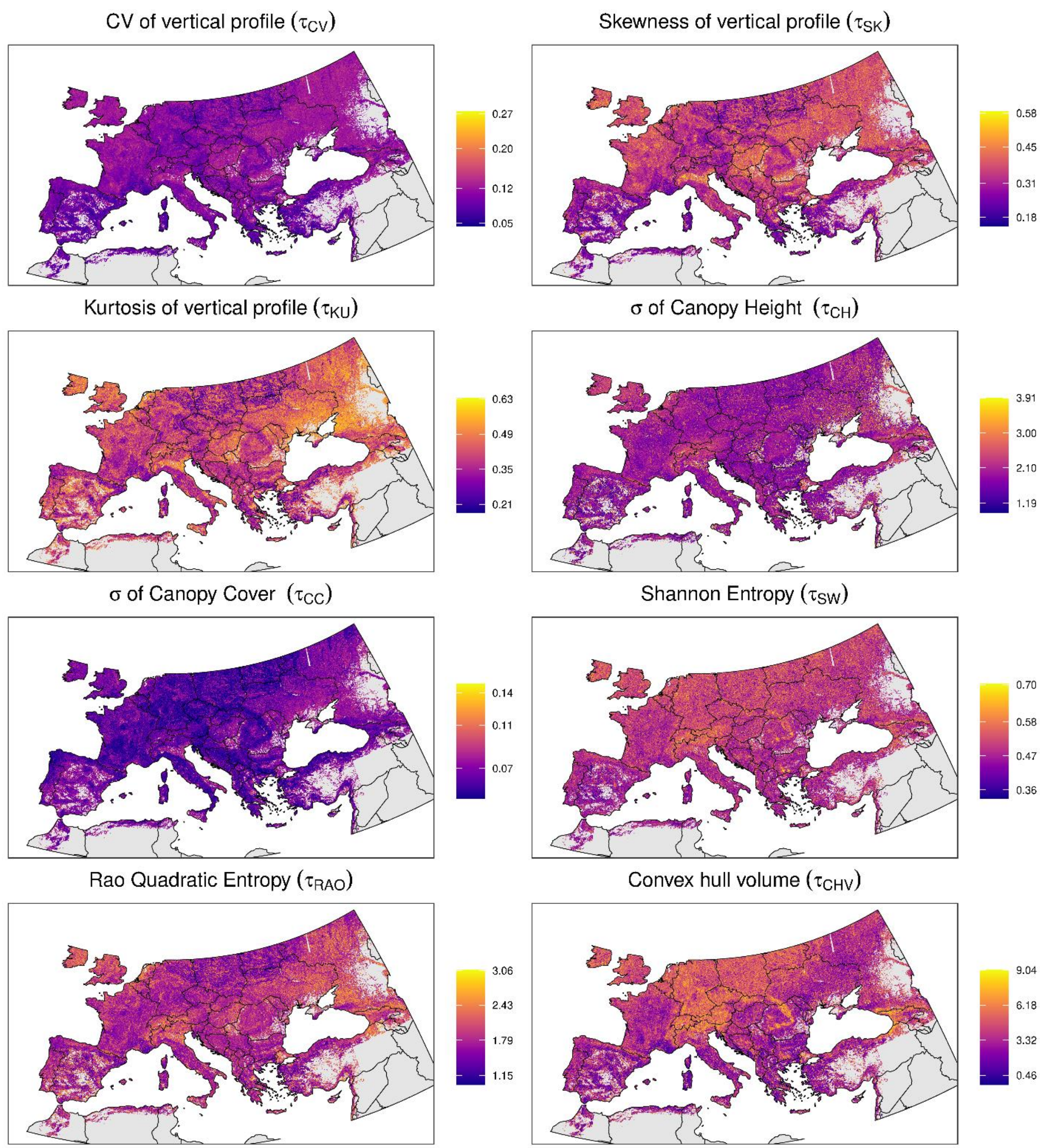

Figure S13 Standard errors of predictions for models trained at 1 km resolution using Random Forest modelling. These errors were calculated using the infinitesimal jackknife method (see Methods for details). The colour palette transitions from purple to yellow, denoting increasing standard error, with warmer colours signifying higher values.